Finite-volume lattice Boltzmann method

Haowen Xi,[1] Gongwen Peng,[2] and So-Hsiang Chou[3]
[1]*Department of Physics and Astronomy, Bowling Green State University, Bowling Green, Ohio 43403*
[2]*Department of Chemical and Petroleum Engineering, University of Pittsburgh, Pittsburgh, Pennsylvania 15260*
[3]*Department of Mathematics and Statistics, Bowling Green State University, Bowling Green, Ohio 43403*
(Received 8 October 1998; revised manuscript received 15 December 1998)

We present a finite-volume formulation for the lattice Boltzmann method (FVLBM) based on standard bilinear quadrilateral elements in two dimensions. The accuracy of this scheme is demonstrated by comparing the velocity field with the analytical solution of the Navier-Stokes equations for time dependent rotating Couette flow and Taylor vortex flow. To demonstrate the flexibility of the scheme, we have also simulated a modified rotating Couette flow, where the inner cylinder has an elliptical shape. The results agree with those obtained from the traditional marker-and-cell method. The FVLBM scheme is applicable to arbitrarily shaped two-dimensional regions, and thus the range of applicability of the lattice Boltzmann method has been significantly extended. [S1063-651X(99)14605-1]

PACS number(s): 47.10.+g, 47.11.+j, 05.20.Dd

In recent years the lattice Boltzmann method (LBM) has attracted much attention in the physics and engineering communities as a possible alternative approach for solving complex fluid dynamics problems. In particular, the inherent parallelism, the simplicity of programming, and the capability of incorporating complex microscopic interactions have made LBM a very attractive simulation method for fluid flow in complex physical systems [1–4].

However, the LBM suffers several limitations. One of these is that the LBM is constructed on a special class of uniform and regular lattices. The limitation of using uniform lattices is particularly severe in many practical applications where the complex geometry of boundaries cannot be well fitted by regular lattices. During the past few years, several researchers were motivated by such considerations and attempted to use irregular lattices. Succi *et al.* [5] were the first to propose a finite volume formulation of the lattice Boltzmann equation (LBE). Quite recently, another elegant finite volume scheme was developed by Chen [6]. In a way similar to the conventional LBMs, He, Luo, and Dembo [7] proposed a model for an arbitrary rectangular mesh. However, the above-mentioned approaches of using irregular meshes are not satisfactory in the sense that the topology of the grids used is not arbitrary. In a recent paper [8], we have proposed a finite-volume scheme using arbitrary two-dimensional linear triangular elements from the point of view of modern finite-volume methods [9,10]. Our finite-volume scheme is applicable to unstructured meshes with arbitrary connectivity.

In this paper, we are going to propose and test a finite-volume scheme on quadrilateral elements. It turns out the extension from linear triangular elements to bilinear quadrilateral elements is not as trivial as one might first think. In fact, a great deal of care has to be made in order to create a simple and practical scheme. Though there are lots of choices of constructing the control volume, we believe that what we present here is the simplest and most efficient model for bilinear quadrilateral elements. In what follows, one could see that our model for the quadrilateral elements looks as if the interpolation *were* linear. In fact, it is not linear but quadratic in nature. This feature makes our model simple and unique.

As emphasized in Refs. [7,11,12], coupling between discretizations of velocity space and physical space is not necessary. We start with lattice Boltzmann equation (LBE) which, after discretizing the velocity space, reads

$$\frac{\partial f_i}{\partial t}+\mathbf{v}_i\cdot\boldsymbol{\nabla} f_i=\Omega_i, \tag{1}$$

where f_i is the particle distribution function associated with motion along the ith direction in velocity space, $\mathbf{v}_i$ the velocity in the ith direction, $i=1,\ 2,\ \ldots,\ N$ with N the number of different velocities in the model, and Ω_i is the collision operator which commonly approximated by the Bhatnagar-Gross-Krook model [13], $\Omega_i=-1/\tau(f_i-f_i^{eq})$, where f_i^{eq} is the local equilibrium distribution and τ the relaxation time. Here we choose the nine velocities for the velocity discretization. The nine discrete velocities are defined by $\mathbf{v}_i=(0,0)$ for $i=0$, $\{\cos[(i-1)\pi/2],\sin[(i-1)\pi/2]\}$ for $i=1\sim4$ and $(\sqrt{2}\{\cos[(i-5)\pi/2+\pi/4],\sin[(i-5)\pi/2+\pi/4]\})$ for $i=5\sim8$. The equilibrium distribution f_i^{eq} is given by

$$f_i^{eq}=w_i\rho[1+\tfrac{3}{2}(\mathbf{v}_i\cdot\mathbf{u})+\tfrac{9}{2}(\mathbf{v}_i\cdot\mathbf{u})^2-\tfrac{3}{2}|\mathbf{u}|^2], \tag{2}$$

where $\rho=\Sigma_i f_i$ and $\rho\mathbf{u}=\Sigma_i f_i\mathbf{v}_i$ are the macroscopic mass density and momentum density respectively, and w_i equals $\frac{4}{9}$ for $i=0$, $\frac{1}{9}$ for $i=1\sim4$, and $\frac{1}{36}$ for $i=5\sim8$.

In Fig. 1, we show the generic situation in which quadrilateral elements surround an interior node of the grid. Here we report a finite-volume method of the cell-vertex type. In this type of formulation, there are two types of grids: the primal grids (or nodes) are those grids P, P_1, P_2, etc., and dual grids (or nodes) are those grids A, B, C, etc., as shown in Fig. 1. The f_is values at the primal nodes are known, and the f_is values at dual nodes are unknown and have to be interpolated from the f_is at the primal nodes using standard interpolation procedures depending on the element types used. For example, linear and ''bilinear'' interpolations

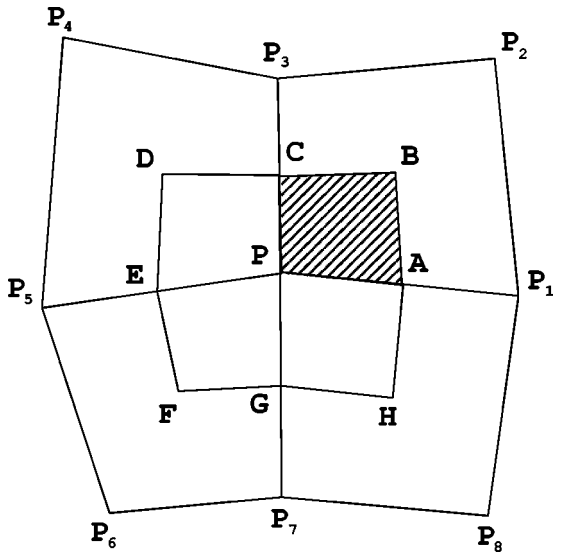

FIG. 1. Diagram of finite elements sharing one common node. Here $P,P_1,P_2,\ldots,P_8$ stand for the mesh grid points. A,B,C,D,E,F,G,H make the edges of the control volume (polygon) over which integration of the PDE of Eq. (1) is performed.

would be applied to the triangular and quadrilateral elements respectively. By ''bilinear'' we mean that a function on a *unit* quadrilateral element $[0\leqslant\xi\leqslant1,\ 0\leqslant\eta\leqslant1]$ has the form of $f(\xi,\eta)=a_0+a_1\xi+a_2\eta+a_3\xi\eta$, where a_0 to a_3 are determined by the function values at the four nodes. Thus the function is linear along constant ξ or η lines. For any quadrilateral element other than a unit quadrilateral element a mapping should be first used to transfer the element on xy plan into a unit one on $\xi\eta$ plan, and therefore the function on a general quadrilateral element typically has terms including all quadratic terms of x^2, y^2, and xy. It should be noted that the function is linear along the images of constant ξ and η lines.

Before we develop the finite-volume scheme, the first question one has to ask is how to choose the control volume $ABC\cdots GH$. Obviously, there are many ways. However, it is very important to find an optimal control volume such that it will lead to a simple and practical finite volume scheme. In the following, we will discuss such choice. The control volume is the polygon $ABC\cdots GH$ surrounding the node P is shown in Fig. 1. We choose A to be the midpoint of edge PP_1, B to be the geometric center of element $PP_1P_2P_3$, and C to be the midpoint of edge PP_3. The coordinates $\mathbf{x}_A$, $\mathbf{x}_B$, and $\mathbf{x}_C$ are given by

$$\mathbf{x}_A=(\mathbf{x}_P+\mathbf{x}_{P_1})/2,\quad \mathbf{x}_B=(\mathbf{x}_P+\mathbf{x}_{P_1}+\mathbf{x}_{P_2}+\mathbf{x}_{P_3})/4,$$

$$\mathbf{x}_C=(\mathbf{x}_P+\mathbf{x}_{P_3})/2. \tag{3}$$

Likewise, D is the center of polygon $PP_3P_4P_5$. The integration volume consists of polygon $PABC$, $PCDE$, $PEFG$, and $PGHA$. It will become obvious later that this control volume has been deliberately designed to give us a simple scheme.

In the following, we focus on the integration over the polygon $PABC$. Similar integrations would be done over all other three polygon centered on P and the results summed. The integration of the first term in Eq. (1) is approximated as

$$\int_{PABC}\frac{\partial f_i}{\partial t}d\sigma=\frac{\partial f_i(P)}{\partial t}S_{PABC}, \tag{4}$$

where S_{PABC} is the area of $PABC$ and $f_i(P)$ is the f_i value at node P. In what follows, the node index is given in parentheses following the f_i values. In the above equation, we have made an approximation that f_i is constant over the area $PABC$ to avoid having to solve a set of equations. This kind of ''lumping'' technique is a common practice in the finite-volume methods [10].

Integration of the second term of Eq. (1) will give fluxes though the four edges PA, AB, BC, and PC,

$$\int_{PABC}\mathbf{v}_i\cdot\nabla f_i d\sigma=\mathbf{v}_i\cdot\int_{AB}f_i d\mathbf{l}+\mathbf{v}_i\cdot\int_{BC}f_i d\mathbf{l}+I_s, \tag{5}$$

where I_s is the fluxes from the internal edges. Since we will sum over all the other polygon like $PCDE$, the net flux through internal edges (PA, PC, PE, and PG) will cancel out. With the assumption of bilinearity of f_is in quadrilateral elements, the flux is given by

$$\int_{PABC}\mathbf{v}_i\cdot\nabla f_i d\sigma=\mathbf{v}_i\cdot\mathbf{n}_{AB}l_{AB}[f_i(A)+f_i(B)]/2+\mathbf{v}_i\cdot\mathbf{n}_{BC}l_{BC}[f_i(B)+f_i(C)]/2+I_s, \tag{6}$$

where $\mathbf{n}_{AB}$ and $\mathbf{n}_{BC}$ are the outward unit vectors normal to the edge AB and BC, respectively, l_{AB} and l_{BC} are the lengths of AB and BC, respectively. $f_i(A)$, $f_i(B)$, and their corresponding equilibrium particle distribution functions are the values of these variables at A and B. These may be obtained by interpolation from the four nodes at element $PP_1P_2P_3$, e.g., $f_i(A)=[f_i(P)+f_i(P_1)]/2$, and $f_i^{eq}(A)=[f_i^{eq}(P)+f_i^{eq}(P_1)]/2$. Note that this seemingly linear interpolation is actually resulting from the bilinear interpolation. This is because we have chosen the control volume such that edges of our control volume (e.g., AB, BC, etc.) are those special lines where the functions are linearly changing along on the $\xi\eta$ plane. In fact, our finite-volume scheme is still quadratic in nature. Of course, one may arbitrarily choose other types of control volume; however, that will result in much more complicated schemes.

Assuming the bilinearity of f_i and f_i^{eq} over the quadrilateral elements, the integration over the collision term of Eq. (1) results in the following formula:

$$-\int_{PABC}\frac{1}{\tau}(f_i-f_i^{eq})d\sigma=-\frac{S_{PABC}}{16\tau}[9\Delta f_i(P)+3\Delta f_i(P_1)+\Delta f_i(P_2)+3\Delta f_i(P_3)], \tag{7}$$

where $\Delta f_i=f_i-f_i^{eq}$, and $f_i(P)$, $f_i(P_1)$, $f_i(P_2)$, and $f_i(P_3)$ and their corresponding equilibrium particle distribution functions are the values of these variables at P, P_1, P_2, and P_3, respectively.

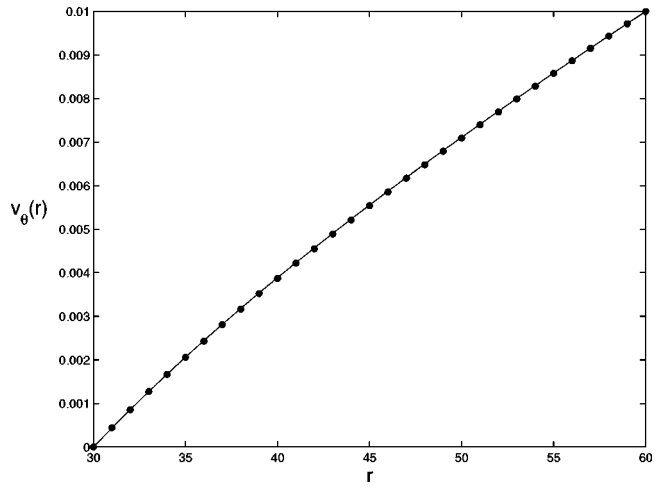

FIG. 2. Numerical velocity profile (data points) in steady state for rotating Couette flow, compared with analytical solution (curve) $v_\theta(r)=V[R_1R_2/(R_2^2-R_1^2)](r/R_1-R_1/r)$.

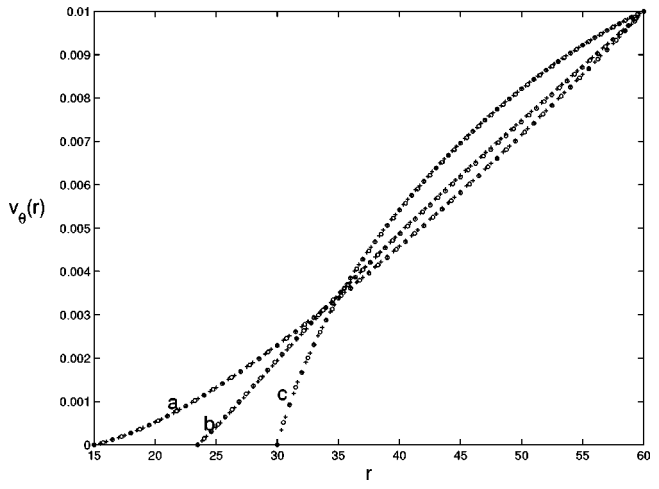

FIG. 3. Numerical velocity profiles in steady state for deformed Couette flow. Velocity was measured along the lines (a) $x=0$, (b) $y=x$, and (c) $y=0$ in the first quarter of the x-y plane. Two sets of symbols stand for finite volume LBM simulations (circles) and MAC simulations (pluses).

With these results, the integration of Eq. (1) over the quadrilateral $PABC$ is complete. The integration over the whole control volume is just the sum of contributions from all these terms over different polygons such as $PCDE$, etc. Therefore, f_i at node P is updated as follows:

$$f_i(P,t+dt)=f_i(P,t)+\frac{dt}{S_P}\left(\sum_{around P}(\text{collisions})-\sum_{around P}(\text{fluxes})\right), \tag{8}$$

where S_P is the total area of the control volume around node P, ''collisions'' and ''fluxes'' refer, respectively, to the finite-volume-integrated contributions from the collision term and fluxes.

To demonstrate the validity of the above scheme, we first simulated the rotating Couette flow, where fluid is contained between two concentric cylinders. The outer cylinder rotates with a constant velocity V, while the inner cylinder is kept at rest. We set the initial conditions for the macroscopic velocity field to be zero. Here we have taken the radii of the two cylinders to be $R_1=30$ and $R_2=60$. The angular velocity of the outer cylinder V to be 0.01. We set fluid density $\rho=1.0$, and relaxation time $\tau=0.5$ with time stepping $\Delta t=0.25$. The mesh size for the system is $N_x\times N_y=180\times 31$, with $\Delta x=\pi/90$ and $\Delta y=1.0$. Note that topologically the computation domain is a rectangular array of points, and we have $\Delta x=\Delta\theta$ and $\Delta y=\Delta r$. In Fig. 2 we show the numerical results of a steady velocity profile and the corresponding analytical solution $v_\theta(r)=V[R_1R_2/(R_2^2-R_1^2)](r/R_1-R_1/r)$. From Fig. 2 one can see that the agreement with the theoretical results is excellent, and the global error was found to be $L_1=10^{-5}$.

To illustrate the flexibility of the FVLBM scheme, we have also simulated a modified rotating Couette flow where the inner cylinder has an elliptical shape. Here the radius of the outer cylinders is still $R_2=60$, and the inner elliptical shape has the form of $(x/15)^2+(y/30)^2=1$. We generate the computation mesh as follows. First, we draw 61 layers with the general equation for the layers $(x/a)^2+(y/b)^2=1$, with $a=15+\frac{3}{4}i$, $b=30+i/2$, where $i=0,1,\ldots,60$ is the layer index. Then, we equally divide the 2π space into 180 parts by drawing straight lines from the origin. The mesh grids have coordinates $x=a\cos(2\pi j/180)$ and $y=b\sin(2\pi j/180)$, with $j=0,1,\ldots,179$. We drive the outer cylinder with the same constant velocity $V=0.01$, while the inner deformed cylinder is still kept at rest. We use the same fluid density $\rho=1.0$ and relaxation time $\tau=0.5$ with time step $\Delta t=0.25$. The spatial steps are $\Delta x=\pi/90$, $\Delta y=0.5$ with total meshes of $N_x\times N_y=180\times 61$ grids are used. Since there is no analytical solution available, we have computed the numerical solution of Navier-Stokes equation using the standard marker-and-cell (MAC) method. In Fig. 3 we show both numerical results and find that they agree extremely well.

In the following, we simulate the evolution of the two-dimensional Taylor vortex flow in a square domain with periodic boundary conditions in both x and y directions. The evolution of velocity field has the analytical solution $\mathbf{u}(x,y,t)=\nabla\times[\phi(x,y,t)\hat{\boldsymbol{e}}_z]$, with $\phi(x,y,t)=(u_0/k_2)\exp[-\nu(k_1^2+k_2^2)t]\cos(k_1x)\cos(k_2y)$. Here $\nabla=\partial_x\hat{\boldsymbol{e}}_x+\partial_y\hat{\boldsymbol{e}}_y$, k_1 and k_2 are the wave number along x and y directions, and ν is the kinematic viscosity of the fluid. The vortex field will decay with exponential rate $\exp[-\nu(k_1^2+k_2^2)t]$. In the simulation, we used wave number $k_1=1$, $k_2=4$. The velocity u_0 was chosen to be 0.01 so that the compressibility of fluid is negligible. We set the density of fluid $\rho=1.0$, and the relaxation time $\tau=10^{-2}$ with time step $\Delta t=10^{-3}$. The space grids $\Delta x=\pi/16$, $\Delta y=\pi/64$, and total meshes $N_x\times N_y=32\times 128$ grids are used. The initial condition for the macroscopic velocity field is $\mathbf{u}(x,y,t=0)=\nabla\times[\phi(x,y,t=0)\hat{\boldsymbol{e}}_z]$ with $\phi(x,y,t=0)=(u_0/k_2)\cos(k_1x)\times\cos(k_2y)$. We have found from this simulation that the kinematic viscosity is equal to $\tau/3$. We did not obtain the numerical viscosity. In Fig. 4 we show the comparison between numerical and analytical solutions for the Taylor vortex flow at different time. Here the analytical curves have used the relation $\nu=\tau/3$. As one can see the agreement between numerical and analytical results is excellent.

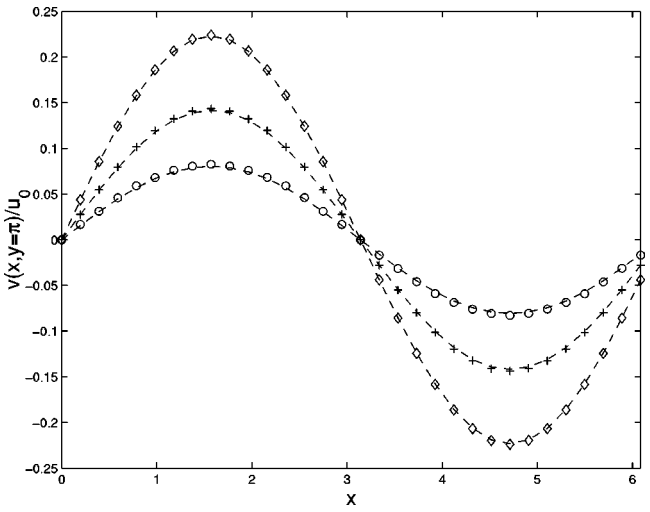

FIG. 4. Numerical velocity $v(x)_{y=\pi}/u_0$ at time t=2, 10, 20 for Taylor vortex flow, compared with the analytical solutions (dashed curves).

It is interesting to make a comparison between the above scheme and the finite-volume scheme of Succi *et al.* [5]. First, our method involved two types of grids, primal (those grids of P, P_1, P_2, etc.) and dual grids (those grids of A, B, C, etc.) as shown in Fig. 1. They only used the primal grids. Second, while they assume linearity of the f_i over primal grid, and only the primal grids are used in the flux calculation. We assume the bilinear of the f_i over primal grids. Our calculation of flux and collision is obtained via integration over control volumes that are made of dual grids. The dual grids that consist of the control volume have been chosen such that the calculation of flux and collision is seemingly linear. In fact, our finite-volume scheme is quadratic in nature. As pointed out in a number of previous studies [5–7], a linear interpolation leads to a numerical viscosity which invalidates the LBE as a useful Navier-Stokes equation solver. Here one should distinguish our model from the linear interpolation model as we emphasized above.

To conclude, we have presented a finite-volume scheme for the LBM using a quadrilateral element that can be applied to unsteady, incompressible fluid flow in a wide variety of shaped boundaries. While our methods follow from an application of finite-volume methods to the LBE, they still keep much of the simplicity of the conventional LBM. This allows the FVLBM to be applied to many interesting systems that so far have been difficult to treat using the conventional LBM. Several applications as well as extensions to three-dimension problems are under investigation and will be reported in subsequent publications.

This work was supported by the PRF under Contract No. 33160-GB9 and the Research Corporation under Grant No. CC4250. The simulations were performed on the SGI Power Challenge at the Ohio Supercomputer Center.

[1] *Lattice Gas Method for Partial Differential Equations*, edited by G. D. Doolen (Addison-Wesley, Redwood City, CA, 1990); *Lattice Gas Methods: Theory, Applications and Hardware*, edited by G. D. Doolen (MIT, Cambridge, MA, 1991).
[2] R. Benzi, S. Succi, and M. Vergassola, Phys. Rep. **222**, 145 (1992).
[3] J. Stat. Phys. **81**, 10 (1995), special issue on lattice-based models and related topics, edited by J. L. Lebowitz, S. A. Orszag, and Y. H. Qian.
[4] S. Chen and G. D. Doolen, Annu. Rev. Fluid Mech. **30**, 329 (1998).
[5] S. Succi, G. Amati, and R. Benzi, J. Stat. Phys. **81**, 5 (1995); F. Nannelli and S. Succi, *ibid.* **68**, 401 (1992).
[6] H. D. Chen, Phys. Rev. E **58**, 3955 (1998).
[7] X. He, L.-S. Luo, and M. Dembo, J. Comput. Phys. **129**, 357 (1996).
[8] G. Peng, H. Xi, C. Duncan, and S. H. Chou, Phys. Rev. E **58**, 4124 (1998).
[9] K. W. Morton, *Numerical Solutions of Convection-Diffusion Problems* (Chapman & Hall, London, 1996).
[10] C. Hirsch, *Numerical Computation of Internal and External Flows, Vol. I: Fundamentals of Numerical Discretization* (Wiley, Chichester, 1988).
[11] S. Chen, D. Martínez, and R. Mei, Phys. Fluids **8**, 2527 (1996).
[12] N. Cao, S. Chen, S. Jin, and D. Martínez, Phys. Rev. E **55**, R21 (1997).
[13] P. L. Bhatnagar, E. P. Gross, and M. Krook, Phys. Rev. **94**, 511 (1954).